PHYSICAL REVIEW A VOLUME 12, NUMBER 4 OCTOBER 1975

Hard-sphere kinetic-theory analysis of classical, simple liquids

Paulo M. Furtado
Department of Nuclear Engineering, Massachusetts Institute of Technology, Cambridge, Massachusetts 02139

Gene F. Mazenko
The James Franck Institute and Department of Physics, The University of Chicago, Chicago, Illinois 60637

Sidney Yip
Department of Nuclear Engineering, Massachusetts Institute of Technology, Cambridge, Massachusetts 02139
(Received 3 March 1975)

The Enskog transport equation, suitably modified to give the proper short-time behavior, is used to study the phase-space density correlation function of a dense fluid of hard spheres. The method of kinetic models is used to obtain numerical solutions for the dynamic structure factor $S(Q,\omega)$; in particular, results are obtained for liquid argon. It is found that for the hard-sphere calculations to give a satisfactory description of the available experimental data produced by computer molecular dynamics studies and neutron inelastic scattering measurements, the factor $g(r_0)$, the pair distribution at contact, should be replaced by a wavelength-dependent quantity. Moreover, the wavelength dependence determined by fitting the experimental data shows a close correlation with the well-known behavior of the static structure factor $S(Q)$. Possible reasons for a nonlocal $g(r_0)$ are discussed.

I. INTRODUCTION

The generalized Enskog equation is the simplest microscopically derived kinetic equation appropriate for describing dense fluids. There have been several recent studies[1-3] of the general properties of this equation; however, no numerical results have been obtained to assess its usefulness as a basis for quantitative calculations. The purpose of this paper is to present the results of the simplest such calculations and to discuss their accuracy in describing the density and current fluctuations in liquid argon.

In using the generalized Enskog equation in any application, one must keep in mind certain obvious limitations of this equation. It is well known that Boltzmann-Enskog–type kinetic equations do not take into account the dynamical processes that lead to the long-time tails which have attracted a good deal of current interest.[4] The theory, as described here, is also tied to the use of hard-sphere interaction; therefore, associated unphysical nonanalyticities[5] in the time dependence of correlation functions can be expected. Nonetheless, the theory is appealing because of its simplicity and because it can be derived microscopically. Since we know what contributions have been neglected, we can systematically improve upon the theory if we desire to do so.[1]

We will analyze the generalized Enskog equation using the method of kinetic models. In this paper we will restrict the analysis to the simplest model calculation. The model used will be called the Q-dependent single-relaxation-time model (QSRT). By taking into account additional matrix elements of the appropriate memory function, we can extend the calculation to higher-order models which eventually should converge numerically to the exact solution.[6,7]

In the present calculation three quantities have to be specified, the structure factor $S(Q)$, the hard-sphere diameter r_0, and the pair distribution function at contact $g(r_0)$. Although the method of Percus-Yevick can be used to determine $S(Q)$ and $g(r_0)$ once r_0 is chosen, this procedure is not likely to yield satisfactory results in comparing calculation against experimental data. The reason is that $g(r_0)$ is a sensitive function of r_0 and has a strong influence on the spectral densities to be computed. We have found that no single value of $g(r_0)$ will lead to satisfactory agreement between the calculated spectra and the neutron and computer molecular dynamics data. Consequently, we will use the experimental $S(Q)$ obtained by neutron diffraction,[8] and then attempt to fit the data by choosing an optimal $g(r_0)$ value at each wave number. We know of no theoretical justification for this empirical procedure. On the other hand, it does give reasonable results and the resulting wave-number variation of the fitted $g(r_0)$ appears to be closely correlated with the structure factor $S(Q)$.

II. GENERALIZED ENSKOG EQUATION

The phase-space correlation function to be analyzed is[9]

$$S(\vec{r}-\vec{r}',\vec{p}\vec{p}',t-t') = \langle \delta f(\vec{r}\vec{p}t)\,\delta f(\vec{r}'\vec{p}'t')\rangle \qquad (2.1)$$

where $\delta f(\vec{r}\,\vec{p}t)$ is the deviation of the phase-space density

$$f(\vec{r}\,\vec{p}\,t)=\sum_{j=1}^{N}\delta(\vec{r}-\vec{R}_j(t))\delta(\vec{p}-\vec{P}_j(t)) \tag{2.2}$$

from its equilibrium value $\langle f(\vec{r}\,\vec{p}t)\rangle = f_0(p)$, and $f_0(p)$ is a Maxwellian normalized to n, the equilibrium number density. In (2.2), $\{\vec{R}_j(t), \vec{P}_j(t)\}$ are the phase coordinates of the particles in the N-particle system. We define the Fourier-Laplace transform of (2.1)

$$S(\vec{Q},\vec{p}\,\vec{p}',z)=i\int d^3r\, e^{-i\vec{Q}\cdot\vec{r}}\int_0^\infty dt\, e^{izt}S(\vec{r},\vec{p}\,\vec{p}',t), \tag{2.3}$$

and consider a kinetic equation of the form

$$[z-(\vec{Q}\cdot\vec{p}/m)]S(\vec{Q},\vec{p}\,\vec{p}',z) - \int d^3q\,\phi(\vec{Q},\vec{p}\,\vec{q},z)S(\vec{Q},\vec{q}\,\vec{p}',z)=-\tilde{S}(\vec{Q},\vec{p}\,\vec{p}'), \tag{2.4}$$

where $\phi(\vec{Q},\vec{p}\,\vec{p}',z)$ is the memory function and $\tilde{S}$ is the initial value of $S(\vec{Q},\vec{p}\,\vec{p}',t)$,

$$\tilde{S}(Q,\vec{p}\,\vec{p}')=f_0(p)\,\delta(\vec{p}-\vec{p}')+f_0(p)f_0(p')[S(Q)-1]/n, \tag{2.5}$$

with $S(Q)$ being the structure factor of the fluid.

For a fluid of hard spheres with diameter r_0 one can show that an approximate expression for the memory function is[1]

$$\phi(\vec{Q},\vec{p}\,\vec{p}',z)=-(\vec{Q}\cdot\vec{p}/m)C(Q)f_0(p) + g(r_0)\phi^{(c)}(\vec{Q},\vec{p}\,\vec{p}'), \tag{2.6}$$

where $C(Q)$ is the direct correlation function

$$nC(Q)=[S(Q)-1]/S(Q) \tag{2.7}$$

and $g(r_0)$ is the pair distribution function at contact. In (2.6) $\phi^{(c)}(\vec{Q},\vec{p}\,\vec{p}')$ is the collision part of the memory function for a low-density system of hard spheres.[6] Inserting (2.6) into (2.4) one finds after some rearrangements

$$[z-(\vec{Q}\cdot\vec{p}/m)]S(\vec{Q},\vec{p}\,\vec{p}',z)+(\vec{Q}\cdot\vec{p}/m)f_0(p)[C(Q)-g(r_0)C_0(Q)]\int d^3q\,S(\vec{Q},\vec{q}\,\vec{p}',z)=ig(r_0)J[S]-\tilde{S}(\vec{Q},\vec{p}\,\vec{p}'), \tag{2.8}$$

where

$$J[S]=r_0^2\int d\Omega_r\, d^3\vec{p}_1[(\vec{p}-\vec{p}_1)\cdot\hat{r}/m]\Theta_-(\hat{r}\cdot(\vec{p}-\vec{p}_1)) \times[f_0(p_1^*)S(\vec{Q},\vec{p}^*\vec{p}',z)-f_0(p_1)S(\vec{Q},\vec{p}\,\vec{p}',z)+e^{+i\vec{Q}\cdot\hat{r}r_0}f_0(p^*)S(\vec{Q},\vec{p}_1^*\vec{p}',z)-e^{-i\vec{Q}\cdot\hat{r}r_0}f_0(p)S(\vec{Q},\vec{p}_1\vec{p}',z)] \tag{2.9}$$

and $C_0(Q)$ is the low-density limit of the direct correlation function. The step function $\Theta_-(x)$ is unity for $x<0$ and vanishes otherwise. The pre- and postcollision momenta of the colliding hard spheres are denoted as $(\vec{p},\vec{p}_1)$ and $(\vec{p}^*,\vec{p}_1^*)$ respectively.

Equation (2.9) differs from the well-known collision integral in the linearized Boltzmann equation for hard spheres only in the presence of the phase factor $\exp(i\vec{Q}\cdot\hat{r}\,\vec{r}_0)$. This result has been previously derived[10,11] and the phase factor was recognized as arising from nonlocal spatial effects in collisions between particles of finite extent. Because the structure of (2.8) closely resembles the Enskog equation,[3,12] we will henceforth refer to (2.8) as the generalized Enskog equation. Whereas the Enskog equation does not give the second frequency moment of the density correlation function correctly, (2.8) does preserve this moment by virtue of the term containing $C(Q)$.

III. KINETIC MODEL REPRESENTATION

We employ the method of kinetic models to obtain the density and current correlation functions from (2.8). We will first cast (2.8) in the form of a kinetic model equation which is amenable to numerical calculations.

The method of kinetic models previously has been used to study (2.8) in the case of dilute gases where $g(r_0)=1$ and $C(Q)$ can be replaced by its low-density expression.[6] Here we will use the same basis functions in defining the matrix elements of the memory function. It will be convenient to introduce in (2.8) the memory functions $\Sigma^{(s)}$ and Σ,

$$\Sigma(\vec{Q},\vec{p}\,\vec{p}')=\Sigma^{(s)}(\vec{Q},\vec{p}\,\vec{p}')+\Sigma^{(c)}(\vec{Q},\vec{p}\,\vec{p}'), \tag{3.1}$$

$$\Sigma^{(s)}(\vec{Q},\vec{p}\,\vec{p}')=(\vec{Q}\cdot\vec{p}/m)C(Q)f_0(p), \tag{3.2}$$

$$g(r_0)C_0(Q)f_0(p)(\vec{Q}\cdot\vec{p}/m)\int d^3q\,S(\vec{Q},\vec{q}\,\vec{p}',z) + ig(r_0)J[S]=\int d^3q\,\Sigma^{(c)}(\vec{Q},\vec{p}\,\vec{q})S(Q,\vec{q}\,\vec{p}',z). \tag{3.3}$$

Now consider the expansion

$$\Sigma(\vec{Q},\vec{\xi}\,\vec{\xi}')=\sum_{\alpha,\beta}\psi_\alpha(\vec{\xi})\psi_\beta(\vec{\xi}')f_0(\xi)\Sigma(\alpha|\beta), \tag{3.4}$$

where

$$\Sigma(\alpha|\beta)=\int d^3\xi\, d^3\xi' f_0(\xi')\psi_\alpha(\vec{\xi})\psi_\beta(\vec{\xi}')\Sigma(\vec{Q},\vec{\xi}\vec{\xi}')\,. \tag{3.5}$$

The basis functions ψ are orthonormalized with weight function $f_0(\xi)$,

$$\psi_{lmn}(\vec{\xi})=(l!\,m!n!)^{-1/2}\overline{H}_l(\xi_x)\overline{H}_m(\xi_y)\overline{H}_n(\xi_z), \tag{3.6}$$

where $\vec{\xi}=\vec{v}/v_0$ and $\overline{H}_l(x)=2^{-l/2}H_l(x/\sqrt{2})$, $H_l(x)$ being the Hermite polynomial. For simplicity each Greek index denotes the integers (lmn). For the memory function $\Sigma^{(s)}$ one has

$$\Sigma^{(s)}(lmn|l'm'n')=-Qv_0nC(Q)\delta_{0l}\delta_{0m}\delta_{1n}\delta_{0l'}\delta_{0m'}\delta_{0n'}\,. \tag{3.7}$$

The matrix elements of $\Sigma^{(c)}$ between hydrodynamic states are given in Table I. In addition, we will need the matrix element

$$\Sigma^{(c)}(011|011)=-16i\sqrt{\pi}nr_0^2v_0g(r_0)\times\left[\frac{4}{15}+\frac{d^2}{dx^2}\left(\frac{1}{x}j_1(x)\right)\right]_{x=Qr_0} \tag{3.8}$$

which is related to the shear-viscosity coefficient.

Given the expansion (3.4) one has a rather standard procedure for constructing kinetic models. Our wave-number–dependent single-relaxation-time description is

$$\begin{aligned}[z-Qv_0\xi_3+i\alpha(Q)]S(\vec{Q},\vec{\xi}\vec{\xi}'',z)&=-\delta(\vec{\xi}-\vec{\xi}'')+f_0(\xi)\Big(\{i\alpha(Q)+\xi_3\Sigma^{(s)}(001|000)\}\int d^3\bar{\xi}\,S(\vec{Q},\vec{\bar{\xi}}\vec{\xi}'',z)\\&+\{\xi_3[i\alpha(Q)+\Sigma^{(c)}(001|001)]+(1/\sqrt{6})(\xi^2-3)\Sigma^{(c)}(001|E)\}\int d^3\bar{\xi}\;\bar{\xi}_3S(\vec{Q},\vec{\bar{\xi}}\vec{\xi}'',z)\\&+\{\xi_3\Sigma^{(c)}(E|001)+(1/\sqrt{6})(\xi^2-3)[i\alpha(Q)+\Sigma^{(c)}(E|E)]\}(1/\sqrt{6})\int d^3\bar{\xi}(\bar{\xi}^2-3)S(\vec{Q},\vec{\bar{\xi}}\vec{\xi}'',z)\Big),\end{aligned} \tag{3.9}$$

where the wavelength-dependent collision frequency $\alpha(Q)$ is set equal to $i\Sigma^{(c)}(011|011)$.

The density correlation function $S(Q,\omega)$ is obtained from

$$S(Q,\omega)=(2/n)\mathrm{Im}[S_1(Q,z)]_{z=\omega+i\epsilon}, \tag{3.10}$$

$$S_1(Q,z)=\int d^3\xi\, d^3\xi' S(\vec{Q},\vec{\xi}\vec{\xi}',z)\,. \tag{3.11}$$

Equation (3.9) can be expressed as a system of coupled equations for

$$S_\beta(Q,z)=\int d^3\xi\, d^3\xi'\,\psi_\beta(\vec{\xi}')S(\vec{Q},\vec{\xi}\vec{\xi}',z) \tag{3.12}$$

with $\psi_1(\vec{\xi})=1$,

$$S_\beta(Q,z)-i\alpha(Q)\sum_{\sigma,\sigma'=1}^{N}D_{\beta\sigma}(Q,z)\gamma_{\sigma\sigma'}(Q)S_{\sigma'}(Q,z)=-nD_{\beta1}(Q,z)S(Q), \tag{3.13}$$

$$D_{\nu\beta}(Q,z)=\int d^3\xi\frac{f_0(\xi)\psi_\nu(\vec{\xi})\psi_\beta(\vec{\xi})}{z-Qv_0\xi_3+i\alpha(Q)}, \tag{3.14}$$

TABLE I. Hydrodynamical matrix elements [a,b] $[nr_0^2v_0g(r_0)]^{-1}\Sigma^{(c)}(\alpha,\beta)$.

α \ β	$\|000\rangle$	$\|001\rangle$	$\|100\rangle$	$\|E\rangle$
$\|000\rangle$	0	0	0	0
$\|001\rangle$	0	$-8i\sqrt{\pi}\left(\frac{1}{3}+\frac{d^2}{dx^2}j_0(x)\right)$	0	$(4\pi/\sqrt{6})j_1(x)$
$\|100\rangle$	0	0	$-4i\sqrt{\pi}\left[\frac{2}{3}-\left(1+\frac{d^2}{dx^2}\right)j_0(x)\right]$	0
$\|E\rangle$	0	$(4\pi/\sqrt{6})j_1(x)$	0	$-\frac{8}{3}i\sqrt{\pi}[1-j_0(x)]$

[a] Here $x=Qr_0$, $|E\rangle=1/\sqrt{3}[|200\rangle+|020\rangle+|002\rangle]$, and $j_i(x)$ are spherical Bessel functions of order i.

[b] Note the misprints in expressions (3.21) and (3.23) in Ref. 6.

$$\gamma_{\nu\beta}(Q) = \delta_{\nu\beta} + \Sigma(\nu|\beta)/i\alpha(Q) . \quad (3.15)$$

We have solved these equations for $S(Q, \omega)$. Following the procedure used by Verlet[13] we obtained $r_0 = 1.02\sigma$, $\sigma = 3.405$ Å, and we have used neutron diffraction measurements[8] to determine $S(Q)$ and $C(Q)$. We then chose $g(r_0)$ to give a good fit to the data at various wavelengths.

Before discussing the fit of the data we note that one does not expect very good agreement in the hydrodynamic regime. The reason is that our simple model does not contain all the matrix elements of the memory function associated with viscous flow and heat conduction. We can calculate the shear viscosity from our model,[14] thus obtaining

$$\eta = \tfrac{4}{15}\sqrt{\pi} m n^2 r_0^4 g(r_0) + m n r_0^2/\alpha(Q=0) . \quad (3.16)$$

However, the result derived from the generalized Enskog equation is[2, 15]

$$\eta_E = [m n r_0^2/\alpha(Q=0)]\{1 + 0.761[\tfrac{2}{3}\pi n r_0^3 g(r_0)]^2 + \tfrac{8}{15}\pi n r_0^3 g(r_0)\} . \quad (3.17)$$

At high densities where $g(r_0)$ is larger than 1 the difference between η and η_E is considerable. The source of the discrepancy is easy to track down. In our model we have assumed that all memory-function matrix elements of the form

$$\int d^3\xi\, d^3\xi'\, \xi_t \Sigma(\vec{Q}, \vec{\xi}\vec{\xi}')\psi_\alpha(\vec{\xi}') f_0(\xi') , \quad (3.18)$$

where ψ_α is a nonhydrodynamical state, are zero. This is only approximately correct, and we see from Eqs. (7.33) and (7.38) in Ref. 1 that it is just these terms that change the shear viscosity from η to η_E. For a better description of the hydrodynamical region we therefore must include more matrix elements in our $S(Q, \omega)$ calculation.

IV. DENSITY FLUCTUATIONS IN LIQUID ARGON

Among the simple liquids currently being investigated liquid argon is the system most extensively studied. Density fluctuations in liquid argon have been measured by means of neutron inelastic scattering[16] in the wave-number range $Q = 1.0$–4.4 Å^{-1} and energy transfer $E = \hbar\omega$ up to 10 meV, and the $S(Q, \omega)$ results analyzed in terms of various generalized hydrodynamics models.[17] Essentially equivalent information, in the form of current correlation $J(Q, \omega) = \omega^2 S(Q, \omega)/Q^2$, has been obtained by computer molecular dynamics experiments[18] and used to test kinetic equation calculations[19] where the memory function $\Sigma^{(c)}$ was modeled in a single-relaxation-time approximation. More recently, computer results on $S(Q, \omega)$ which extend to Q as small as 0.183 Å^{-1} have been reported,[20] and these were used to assess the quantitative effects of potential-energy fluctuations in the kinetic equation approach.[21]

In the present calculations we are mostly concerned with the behavior of $S(Q, \omega)$ as revealed in the neutron and computer data. Using (3.9) we have computed $S(Q, \omega)$ according to the parameter values shown in Table II. The value of the hard-sphere diameter r_0 was found by fitting the analytical solution of the Percus-Yevick equation to the structure factor $S(Q)$ generated by computer experiments.[13] At a given Q we choose $g(r_0)$ on the basis that both $S(Q, \omega = 0)$ and the full width at half-maximum (FWHM) of $S(Q, \omega)$ are in reasonable agreement with the data. This procedure is not precise because these two quantities cannot be simultaneously fitted exactly. The general behavior of the fitted $g(r_0)$, labeled $\chi(Qr_0)$, is shown in Fig. 1 along with the structure factor $S(Q)$. We have also used the relation[22]

$$g(r_0) = \frac{1}{4\eta}\left(\frac{1+\eta+\eta^2}{(1-\eta)^3} - 1\right) \quad (4.1)$$

with $\eta = \frac{1}{6}\pi n r_0^3$ to find r_0 for a given value of $g(r_0)$. It can be verified using $\chi(Qr_0)$ in Fig. 1 that r_0 is

TABLE II. Parameters used in the analysis of neutron-scattering experiments on liquid argon.

m (g)	$0.597\,17 \times 10^{-22}$
n (cm^{-3})	0.0213×10^{24}
β^{-1} (erg)	0.1176×10^{-13}
η_s (P)	0.277×10^{-2}
r_0 (Å)	3.4731

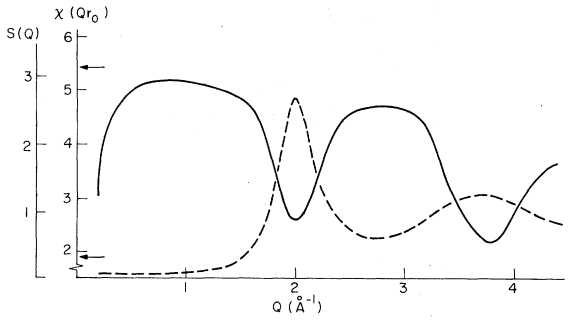

FIG. 1. Wave-number dependence of the fitted $g(r_0)$, labeled parameter $\chi(Qr_0)$, for liquid ^{36}Ar at 85.2 °K (solid line). The experimental structure factor $S(Q)$ is shown as the dashed line. The values of the experimental radial distribution function at $r_0 = 3.4731$ Å and that found from the hard-sphere equation of state (4.1) are indicated by the lower and upper arrows, respectively. In all the calculations presented below the empirically determined parameter $\chi(Qr_0)$ has been used.

a very slowly varying function of Q. Thus our physical picture of a hard-sphere fluid is still reasonable.

It is noteworthy that the wave-number dependence of $\chi(Qr_0)$ bears such a close correlation with the structure factor $S(Q)$. As a purely speculative comment we feel this behavior is consistent with the intuitive expectation that effective collision rates ought to be relatively lower at those wavelengths in the vicinity of near-neighbor separations. If this is the case, then the effect is more related to the geometry of molecular packing than any consequences of dynamics such as those due to attractive forces.

The spectra of $S(Q, \omega)$ calculated using the fitted $g(r_0)$ are shown in Figs. 2–4. The results are compared with neutron scattering data and the more recent computer results. In Fig. 5 we show the wave-number dependence of $S(Q, \omega = 0)$, FWHM, the maximum value of $J(Q, \omega)$, and the position where the maximum occurs, $E_{\max} = \hbar\omega_{\max}$. The numerical values of these quantities are given in Table III where they have been used to compute the root-mean-square deviation σ (Table IV). For $Q < 1.0$ Å^{-1} we did not try to generate the current correlation function because of the uncertainties from reading the $S(Q, \omega)$ values from the graphs of Ref. 20.

We can compare our results using the empirically determined $g(r_0)$ with those obtained by using a constant value of $g(r_0)$. Once r_0 is fixed $g(r_0)$ can be calculated in two different ways. Using expression (4.1) and $r_0 = 3.4371$ Å we find $g(r_0) = 5.43$. On the other hand, a value of 1.88 is obtained from the experimental pair distribution[8] at the same r_0 value. In Table III we also show the results obtained with $g(r_0)$ equal to 1.88 and 5.43. One can observe that the lower $g(r_0)$ value gives better agreement at large Q and ω, whereas for smaller Q and ω the higher value of $g(r_0)$ gives better results. By giving $g(r_0)$ a Q dependence we obtain significant improvement in the low-frequency region, a region where $S(Q, \omega)$ has most of its weight.

Inspection of the calculated $S(Q, \omega)$ and $J(Q, \omega)$ shows that neither of the two constant values of $g(r_0)$ give completely satisfactory results over the range of Q values where either neutron or computer data are available. The desired behavior of $S(Q, \omega)$ seems to be intermediate to those calculated using these two $g(r_0)$ values. By fitting $g(r_0)$ we find that the modified Enskog equation can account for all the interesting features of $S(Q, \omega)$ observed by neutron scattering and computer experiments. From Fig. 2 we see that the onset of a resonant mode or the presence of collective excitations is predicted correctly by the present kinetic theory approach. At the larger wave numbers the calculations are generally in good agreement as can be seen in Fig. 3. When the spectra are displayed at constant frequencies (Fig. 4) we see that the hard-sphere kinetic equation with a fitted $g(r_0)$ gives a rather good account of the Q dependence which varies in a subtle way with ω. The quantitative agreement achieved in Fig. 5 and Table III is comparable to the generalized hydrodynamics calculations where a characteristic re-

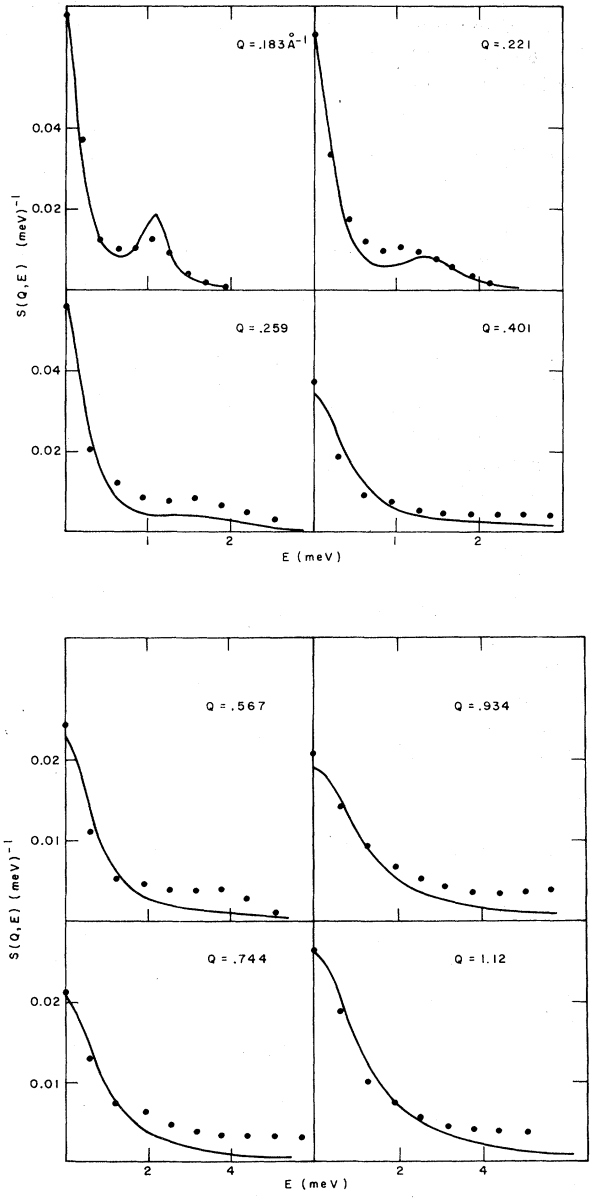

FIG. 2. Dynamical structure factor $S(Q, E)$ of liquid ^{36}Ar at 86.5 °K at eight values of wave-number transfer Q. Solid curves, QSRT calculations; circles, computer molecular dynamics data.[20]

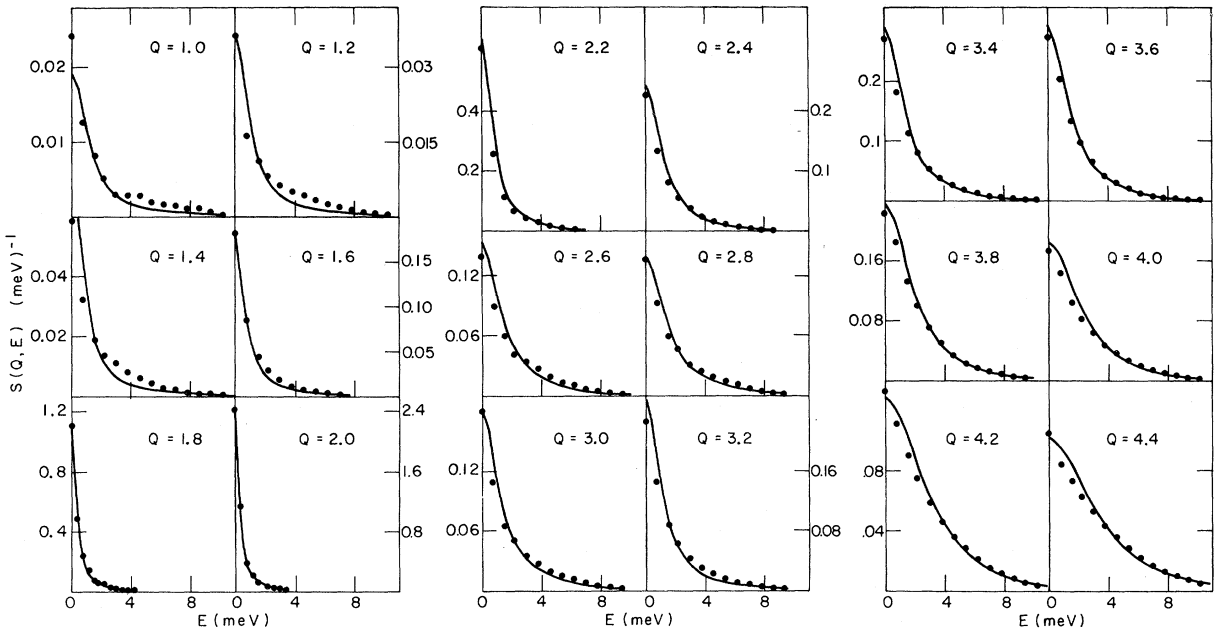

FIG. 3. Dynamical structure factor of liquid ^{36}Ar at 85.2 °K at eighteen values of wave-number transfer. Solid curves, QSRT calculations; circles, coherent neutron inelastic scattering data.[16]

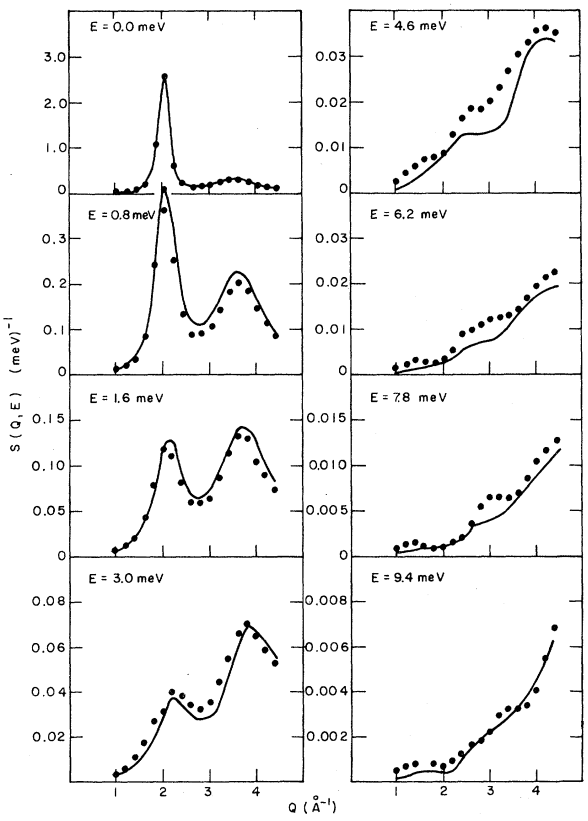

FIG. 4. Dynamical structure factor of liquid ^{36}Ar at 85.2 °K at eight values of energy transfer E. Solid curves, QSRT calculations; circles, coherent neutron inelastic scattering data.[16]

laxation time was used as a fitting parameter.[17] Our agreement is also comparable to that achieved in kinetic equation analysis using a modeled memory function.[19] On the other hand, a formulation taking into account potential-energy density fluctuations[21] apparently gives a somewhat finer description of the long-wavelength region than our results.

V. DISCUSSION

In this paper we have applied a kinetic equation for hard-sphere fluids to the analysis of thermal fluctuations in simple liquids. Our results on liquid argon show that over a wavelength region where the density correlation function can take on quite different behavior the theory is quantitatively successful if the factor $g(r_0)$ is reinterpreted as a wavelength-dependent quantity. Because our particular fitting procedure is neither operationally precise nor theoretically well founded, the results shown in Fig. 1 should be regarded as having mainly qualitative significance. Nonetheless, we think that the fitted values of $g(r_0)$ are reasonable because they lie within the estimates obtained from the Percus-Yevick equation of state and the experimental $g(r)$ for liquid argon. Moreover, we find that the wavelength variation of the fitted $g(r_0)$ is very closely related to the well-understood structure of $S(Q)$. Even though we have not been able to explain this correlation, we be-

lieve this is an important observation, one worthy of further investigation.

We can think of at least three possible sources which can contribute to the manifestation of a wavelength-dependent $g(r_0)$. All these effects arise from the approximations we have made in obtaining the numerical results; the approximations are (1) the replacement of the generalized Enskog equation by the single relaxation time model QSRT, (2) the neglect of more complicated collision processes, and (3) the representation of liquid argon as hard-sphere fluid.

The use of model QSRT was motivated mostly by its mathematical simplicity. While we do not think this model is the reason for the behavior of the fitted $g(r_0)$, we expect that it will begin to break down as we approach the hydrodynamical regime because of the neglect of certain off-diagonal matrix elements of the memory function. The effects of such matrix elements in determining the shear viscosity have already been noted in Sec. III. Since the relaxation time in the model was chosen to give the correct shear viscosity, we expect the model to be even more inadequate in calculating the thermal conductivity because in the low-density limit the model would have given a conductivity differing from the correct value by the factor of $\frac{3}{2}$. The inadequacies of QSRT can be eliminated by working with extended kinetic models which include enough matrix elements to ensure the correct Enskog transport coefficients. We know the Q dependence of each matrix element[6] but it is difficult to anticipate their effects on $S(Q, \omega)$ in the range of Q values we have considered here. Higher-order model calculations would be of considerable interest especially when one can determine whether the behavior of $g(r_0)$ in Fig. 1 continues to give a good fit of the data.

Approximation (2) is concerned with the inadequacy of the generalized Enskog equation in describing the dynamics of dense hard-sphere fluids. It is clear that (2.8) describes only binary collisions and therefore does not take into account recollision processes known to be important at high fluid densities. In particular the Enskog expressions for the transport coefficients must be modified by the Alder factor,[23] $\eta = A(n r_0^3)\eta_E$. This correction factor is primarily due to the recollision processes and can be quite important. We find for $n r_0^3 = 0.892$ that $A = 1.403$.

One can modify (2.8) by adding to the memory

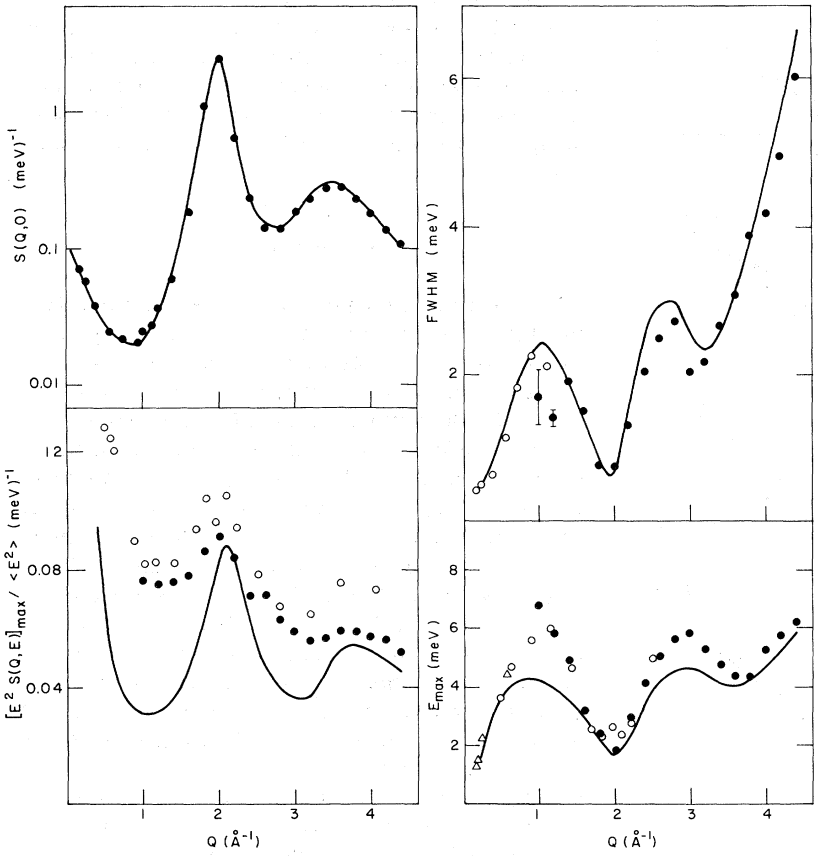

FIG. 5. Wave-number variation of $S(Q, 0)$, the full width at half maximum (FWHM) of the dynamical structure factor, the maximum value of the longitudinal current correlation, and the peak frequency of longitudinal current correlation. In all cases solid curve denotes QSRT calculations. In $S(Q, 0)$ the circles represent the computer molecular dynamics data[20] for $Q \leq 1.0$ Å^{-1} and for $Q > 1.0$ Å^{-1} they represent the neutron data.[16] In FWHM open and solid circles are computer[20] and neutron[16] data respectively. The indicated error bars are those given in Ref. 16. In $[E^2 S(Q, E)]_{\max}/\langle E^2 \rangle$ the open circles are computer data[18] and solid circles are neutron data.[16] In $E_{\max}$ the open triangles[20] and open circles[18] denote computer data while solid circles are neutron data.[16]

TABLE III. Parameters used to characterize the dynamical structure factor. The experimental data are from Refs. 16 and 20. Columns (1) and (2) give the results of the QSRT calculation for $g(r_0) = 1.88$ and 5.43 respectively; column (3) is the QSRT calculation when the parameter $\chi(Qr_0)$ is used.

	FWHM (meV)				$S(Q,0)$ (meV^{-1})				$[J(Q,E)]_{max}/\langle E^2\rangle$ (meV^{-1})				E_{max} (meV)			
Q (Å^{-1})	Expt.	1	2	3	Expt.	1	2	3	Expt.	1	2	3	Expt.	1	2	3
0.183	0.423	0.56	0.23	0.40	0.068	0.043	0.133	0.066								
0.221	0.444	0.73	0.32	0.421	0.063	0.033	0.098	0.061								
0.259	0.491	0.97	0.36	0.494	0.056	0.027	0.075	0.057								
0.401	0.634	2.13	0.77	0.908	0.037	0.015	0.039	0.034								
0.567	1.172	5.6	1.33	1.45	0.024	0.010	0.025	0.023								
0.744	1.806	6.4	1.72	1.812	0.021	0.009	0.022	0.021								
0.934	2.25	7.78	2.19	2.295	0.021	0.008	0.020	0.019								
1.0	1.70	8.12	2.26	2.447	0.024	0.008	0.020	0.019	0.076	0.081	0.029	0.031	6.75	4.0	4.2	4.2
1.2	1.42	6.8	1.92	2.143	0.036	0.016	0.038	0.035	0.075	0.078	0.029	0.031	5.80	3.8	3.8	3.8
1.4	1.90	5.27	1.67	1.865	0.059	0.034	0.079	0.072	0.076	0.083	0.033	0.036	4.90	3.5	3.6	3.6
1.6	1.50	3.4	1.32	1.511	0.180	0.095	0.205	0.179	0.078	0.091	0.040	0.046	3.1	2.7	3.4	3.2
1.8	0.75	1.45	0.68	0.871	1.10	0.632	1.231	0.952	0.086	0.097	0.049	0.063	2.4	2.1	2.8	2.2
2.0	0.74	0.82	0.47	0.626	2.40	2.246	3.886	2.594	0.091	0.099	0.057	0.085	1.8	1.4	2.0	1.6
2.2	1.32	1.87	1.05	1.597	0.62	0.579	0.946	0.651	0.084	0.094	0.057	0.084	2.9	2.4	2.4	2.2
2.4	2.03	3.70	1.88	2.477	0.225	0.179	0.300	0.239	0.071	0.083	0.048	0.062	4.1	3.4	3.4	3.4
2.6	2.50	5.0	2.36	2.936	0.139	0.102	0.180	0.151	0.071	0.073	0.039	0.048	5.0	4.1	4.2	4.2
2.8	2.72	5.4	2.42	2.937	0.135	0.091	0.166	0.141	0.063	0.064	0.034	0.040	5.6	4.4	4.8	4.6
3.0	2.04	4.75	2.21	2.618	0.179	0.114	0.209	0.180	0.059	0.059	0.031	0.036	5.8	4.6	4.8	4.6
3.2	2.17	4.0	1.94	2.349	0.225	0.168	0.301	0.254	0.056	0.057	0.031	0.037	5.25	4.3	4.8	4.4
3.4	2.64	3.5	1.82	2.724	0.270	0.237	0.408	0.289	0.057	0.057	0.032	0.046	4.75	4.0	4.6	4.0
3.6	3.08	3.6	2.0	3.095	0.273	0.258	0.418	0.291	0.059	0.058	0.035	0.051	4.35	4.0	4.4	4.0
3.8	3.88	4.21	2.44	3.934	0.223	0.225	0.343	0.236	0.059	0.058	0.038	0.055	4.25	4.2	4.6	4.2
4.0	4.2	5.2	3.09	4.593	0.173	0.168	0.248	0.184	0.057	0.057	0.038	0.051	5.25	4.6	5.0	4.6
4.2	4.97	6.52	3.79	5.788	0.133	0.118	0.176	0.129	0.056	0.053	0.035	0.049	5.70	5.4	5.6	5.4
4.4	6.04	7.50	4.39	6.611	0.105	0.093	0.142	0.102	0.052	0.050	0.032	0.045	6.20	6.0	6.2	5.8

TABLE IV. Standard deviation $\sigma(\%)$ for the parameters shown in Table III.

	σ (%)								
	$Q = 0.18$–4.4 Å^{-1}			$Q = 1.0$–4.4 Å^{-1}			$Q = 1.6$–4.4 Å^{-1}		
	(1)	(2)	(3)	(1)	(2)	(3)	(1)	(2)	(3)
$S(Q, 0)$	33.7	38.5	8.5	31.4	36.8	9.6	24.0	38.6	7.0
FWHM	131	23.0	19.8	148	24.1	20.6	71.5	23.0	14.4
E_{max}	...	...	...	19.9	16.4	18.5	15.2	10.2	13.8
$[J(Q, E)]_{max}/\langle E^2 \rangle$	...	...	...	8.0	44.6	32.0	8.2	39.5	24.2

function $\Sigma^{(c)}$ the appropriate contribution from ring collisions.[1] The calculation of $S(Q, \omega)$ using such a kinetic description would become much more difficult, but the results would be extremely interesting and can tell us much about the relation between molecular collisions and the dynamical properties of a many-body system.

Approximation (3) is of quite different nature, and like approximation (2) it lies outside the scope of the present generalized Enskog equation. It is widely known that hard-sphere systems show certain pathological properties because of the nature of the interaction potential. For example, the sum rules for a hard-sphere system are intrinsically different from those for a Lennard-Jones system,[5,12] and the effects manifest in the very short-time behavior of the time autocorrelation functions. A somewhat more subtle difference occurs in the potential-energy contributions to thermal fluctuations. Although these effects would not be present in a hard-sphere fluid, they can be treated by considering a memory function like that given in Eq. (6.37) of Ref. 1. Recently Jhon and Forster[21] have shown that the effects of potential-energy contributions can be important in the analysis of the liquid-argon data at long wavelengths.

It is clear from our comments that to assess the effects of approximations (2) and (3) additional data on time correlation functions are needed. It would be immensely helpful if computer molecular dynamics results on hard-sphere fluids of comparable density and temperature were available.[24] The analysis of such data using the method described here will indicate the importance of the more complex collision processes, and a comparison of the computer results for hard spheres and Lennard-Jones atoms would be most enlightening in delineating those effects that can be attributed to the details of the interaction potential.

ACKNOWLEDGMENT

This work was supported by a grant from the National Science Foundation, GK-32908.

[1] G. F. Mazenko, Phys. Rev. A 9, 360 (1974).
[2] H. H. V. Könijnendijk and J. M. J. van Leeuwen, Physica 64, 342 (1973).
[3] J. Sykes, J. Stat. Phys. 8, 279 (1973).
[4] B. J. Alder and T. E. Wainwright, Phys. Rev. Lett. 18, 988 (1967); Phys. Rev. A 1, 18 (1970); T. E. Wainwright, B. J. Alder, and D. M. Gass, Phys. Rev. A 4, 233 (1971); see also Ref. 23.
[5] V. F. Sears, Phys. Rev. A 5, 452 (1972); see also Ref. 11.
[6] G. F. Mazenko, T. Y. C. Wei, and S. Yip, Phys. Rev. A 6, 1981 (1972).
[7] A. Sugawara and S. Yip, Phys. Fluids 11, 925 (1968).
[8] J. L. Yarnell, M. J. Katz, R. G. Wenzel, and S. H. Koenig, Phys. Rev. A 7, 2130 (1973).
[9] We will follow the notation used in Ref. 6.
[10] J. M. J. van Leeuwen and S. Yip, Phys. Rev. 139, A1138 (1965).
[11] J. L. Lebowitz, J. K. Percus, and J. Sykes, Phys. Rev. 188, 487 (1969).
[12] E. P. Gross and W. Wisnivesky, Phys. Fluids 11, 1387 (1968).
[13] L. Verlet, Phys. Rev. 165, 201 (1968).
[14] G. F. Mazenko, Ph. D. thesis (MIT, 1971) (unpublished).
[15] J. O. Hirschfelder, C. F. Curtiss, and R. B. Bird, *Molecular Theory of Gases and Liquids* (Wiley, New York, 1954).
[16] K. Sköld, J. M. Rowe, G. Ostrowsky, and P. D. Randolph, Phys. Rev. A 6, 1107 (1972).
[17] J. M. Rowe and K. Sköld, in *Neutron Inelastic Scattering* (International Atomic Energy Agency, Vienna, 1972), p. 413.
[18] A. Rahman, in *Neutron Inelastic Scattering* (International Atomic Energy Agency, Vienna, 1968), Vol. I, p. 561.
[19] J. J. Duderstadt and A. Z. Akcasu, Phys. Rev. A 1, 905 (1970).
[20] D. Levesque, L. Verlet, and J. Kurkijarvi, Phys. Rev. A 7, 1690 (1973).
[21] M. S. Jhon and D. Forster, Phys. Rev. A 12, 254 (1975).
[22] N. F. Carnahan and K. E. Starling, J. Chem. Phys. 51, 635 (1969).
[23] B. J. Alder, D. M. Gass, and T. E. Wainwright, J. Chem. Phys. 53, 3813 (1970).
[24] Data of this type are currently being generated and will appear in the literature shortly; B. J. Alder (private communication).